

Theoretical Studies of Manganese and Iron Superoxide Dismutases: Superoxide Binding and Superoxide Oxidation

Isabel A. Abreu, José A. Rodriguez,* and Diane E. Cabelli*

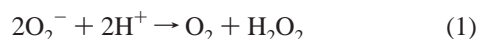
Chemistry Department, Brookhaven National Laboratory, Upton, New York 11973

Received: May 9, 2005; In Final Form: September 14, 2005

Density-functional calculations indicate that the second sphere of coordination around the metal centers of manganese and iron superoxide dismutases (MnSODs and FeSODs) plays an important role in the binding of O_2^- . In these systems, O_2^- prefers to bind to Mn or Fe in end-on configurations. For human and *E. coli* MnSODs, the bound O_2^- forms hydrogen bonds with the tyrosine and glutamine amino acid residues in the second sphere of coordination. In the cases of *E. coli* and *T. elongates* FeSODs, hydrogen bonding occurs between the bound O_2^- and the tyrosine amino acid only because the glutamine is too far away for an effective bonding interaction. The manner in which the O_2^- binds to the metal center in MnSODs and FeSODs can affect the rate of subsequent protonation and determine the mechanism for the formation of H_2O_2 . Both Mn- and Fe-containing superoxide dismutases contain a metal-bound solvent molecule that has been suggested to be involved in the uptake of a H^+ upon reduction of the metal center [Bull, C.; Fee, J. A. *J. Am. Chem. Soc.* **1985**, *107*, 3295; Miller, A.-F.; Padmakumar, K.; Sorkin, D. L.; Karapetian, A.; Vance, C. K. *J. Inorg. Biochem.* **2003**, *93*, 71]. Using density-functional theory, we confirm this suggestion and show the involvement of the second sphere of coordination in the process. We show that the oxidation of superoxide by Mn- or Fe-containing superoxide dismutases is facilitated by a cooperative effect between superoxide binding, protonation of the OH^- bound to the metal, and electron transfer from the superoxide molecule to the oxidized metal. In particular, proton transfer through tyrosine-34 on the absence of a bound superoxide is uphill while, once superoxide is bound, the energetic barrier is lowered. It is this barrier that likely keeps the resting state (Mn(III)SOD) of the enzyme with a bound hydroxide, instead of a water. This work provides a model for the mechanism of reaction of superoxide with the oxidized form of the metal within Mn- and FeSODs.

Introduction

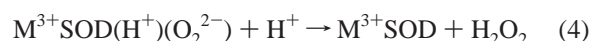
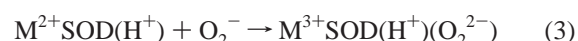
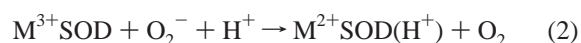
Superoxide dismutases (SODs) are metalloenzymes that protect biological systems against oxidative damage by catalyzing the dismutation of superoxide anions (O_2^-) to molecular oxygen and hydrogen peroxide according to a one-electron redox cycle:^{1–3}



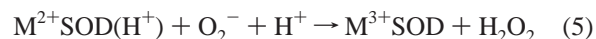
This redox process can be carried out at Fe, Mn, Cu, or Ni metal centers.^{2,4} MnSODs and FeSODs have received much attention^{1,2,3,5–9} because MnSODs are found in many bacteria and in the mitochondria of eukaryotic cells while FeSODs are found in prokaryotes and plants.⁴ The Mn- and Fe-containing SODs possess a very similar protein structure, with almost identical first and second sphere coordination shells.^{1,4–6} Upon isolation, the metal centers are generally in a +3 formal oxidation state and bound in a trigonal bipyramidal geometry with three histidines, one aspartate, and a water or OH^- molecule as ligands.^{1,3,5,6} The OH^- molecule is protonated to a water molecule when the metal is in its reduced state (+2 formal oxidation state).^{1b,3b}

Despite these structural similarities, the enzymes exhibit metal ion specificity (i.e., Mn incorporated into the FeSOD protein matrix (Mn(Fe)SOD) is catalytically inactive, as is Fe(Mn)-

SOD)¹⁰ and follow different mechanisms for the dismutation of O_2^- anions.^{1,6} The exceptions to this metal specificity are the “cambialistic” enzymes that can function using either manganese or iron as the redox active metal. Both MnSODs and FeSODs catalyze the disproportionation of superoxide by an alternate reduction/oxidation of the metal:^{1,2a,3}



In the case of the Mn-containing enzymes, a parallel pathway for conversion of superoxide to hydrogen peroxide has been observed:^{2a,5,7}



Several hypotheses have been proposed to explain the differences in the behavior of the MnSODs and FeSODs.^{1,2a,3,4–6,8,10} Recent studies suggest that the key may be in the particular configuration of the amino acids located in the second sphere of coordination around the metal centers, in particular the tyrosine and glutamine that have been postulated to play a role in the proton transfer.^{3,5,6} Therefore, it is very important to establish how these amino acids affect the bonding of O_2^- to the Mn and Fe sites of the SODs.

* Corresponding authors. E-mail: rodriguez@bnl.gov (J.A.R.); cabelli@bnl.gov (D.E.C.).

In reactions 2–5, O_2^- can bind to the metal centers of the protein via end-on (one Mn–O or Fe–O bond) or side-on (two Mn–O or Fe–O bonds) conformations.^{5a,9,11–13} In principle, the way in which the molecule binds to the metal centers can affect the rate of subsequent protonation and determine the mechanism for the formation of H_2O_2 in MnSODs.^{2a,5,13} These are complex systems because the amino acids in the second sphere of coordination around Mn and Fe can interact with O_2^- through H bonding and provide the protons necessary for reactions 4 and 5. In this paper, we use density-functional (DF) calculations to study the bonding of O_2^- to MnSODs and FeSODs and the mechanism by which OH^- is protonated to water upon reduction of the metal in the center and how this affects the oxidation of O_2^- by MnSODs and FeSODs. We have also studied the changes that occur when the tyrosine located in the second coordination sphere is deprotonated or modified to phenylalanine and whether the glutamine in the second coordination sphere plays a role at all.

Theoretical Methods

The DMol³ code¹⁴ was employed in the present study. It allows modeling the electronic structure and energetics of molecules, proteins, and surfaces using DF theory.^{12,15–18} In the past, DF calculations have been used to study proton transfer and relative pK_a 's in MnSODs and FeSODs,^{6,8} and the bonding of O_2 and O_2^- species to iron cations in [2Fe–2S]-protein clusters¹² and the superoxide reductase (SOR) enzyme.¹³ Here, all the electrons of H, C, N, O, Mn, and Fe were included in the calculations explicitly. The linear combinations of localized numerical atomic orbitals used as basis sets are designed to give maximum accuracy for a given basis set size.¹⁴ In the present DMol³ calculations, we used a numerical basis set that describes the orbitals in the valence shell with double numeric functions together with polarization and/or diffuse functions. It has an accuracy higher than that of double- ζ Slater or double- ζ Gaussian basis sets. When a more extended basis set was tested in benchmark calculations (for example, $Mn^{2+} + O_2^-$ binding), no remarkable changes appeared. Since the numerical basis set used here is of very high quality,¹⁴ the basis set superposition error (BSSE) should be on the order of <10% of the reported bonding energies.^{15–17}

The structural parameters and bonding energies reported in the Results section were obtained using the generalized gradient approximation (GGA) with Becke-88 for exchange¹⁹ and Perdew-91 for correlation.²⁰ Our major interest here is in qualitative trends in the calculated bonding energies,^{20,23,24} not in absolute values. (The accuracy of DFT-GGA bonding energies is frequently on the order of 5 kcal/mol, and this type of quantum-chemical calculation is very powerful for studying trends in chemical reactivity.^{20,23,24}) The basis set and functionals used in this work reproduced very well the experimental geometries known for the metal centers in Mn(II)SODs and Fe(II)SODs or Mn(III)SODs and Fe(III)SODs (see below), gave the type of interactions observed in other theoretical studies for the bonding of O_2^- to FeSODs,¹³ and predicted bonding energies for CO and H_2O on $FeS_2(100)$ that were within 3 kcal/mol of the experimental values.¹² We calculated homolytic bond dissociation energies for an O–H in H_2O (122 kcal/mol) and the O–H in phenol (84 kcal/mol) that are very close to those found experimentally and in other theoretical calculations (~118 and 87 kcal/mol, respectively).^{17b}

For each of the examined systems, a Mulliken population analysis²¹ was performed to estimate the partial charge on each atom and variations in charge distribution when going from

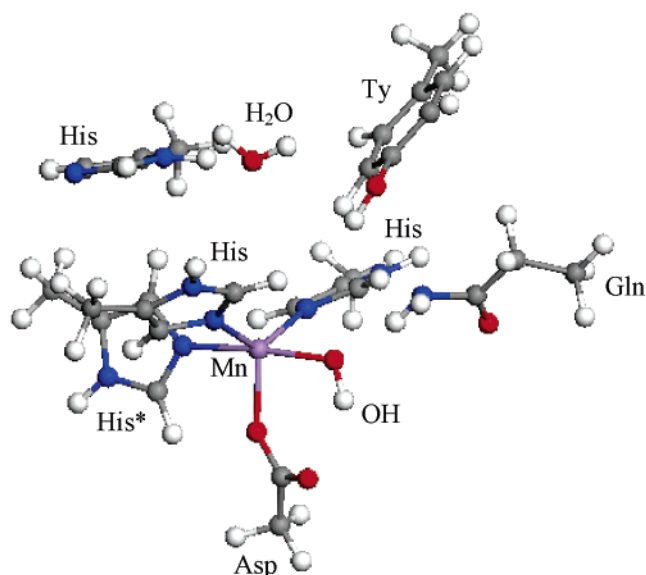


Figure 1. Model used to study the interaction of O_2^- with Mn(III)-SODs. The different colors denote the following: magenta, Mn; gray, carbon; white, hydrogen; dark blue, nitrogen; red, oxygen. In the model are included ligands in the first sphere of coordination of the metal center (three histidines, one aspartate, and an OH group), and amino acids in the second sphere of coordination (one glutamine, one tyrosine, and one histidine). A similar model was used to study Fe(III)SODs. In the cases of Mn(II)SODs and Fe(II)SODs, a water molecule was bonded to the metal center instead of an OH group. Once bound, the O_2^- anion interacted directly with the metal center and through H bonds with the His* (less stable configuration) or with the Tyr and Gln (more stable conformation).

MnSODs to FeSODs. The Mulliken population analysis has well-known approximations,²⁷ and in many cases it has proven to be useful for examining correlations between charge distribution and chemical reactivity.^{17,22}

At the present time, it is impossible to do first-principles density-functional calculations for large biomolecules due to the requirements of computer time. To overcome this problem, simplified models are frequently used that contain the active metal center and the amino acids in its first and second spheres of coordination.^{2c,6,8,12,13,23} Figure 1 shows the model used to study the bonding of O_2^- to MnSODs and FeSODs. It includes the most important ligands around the Mn and Fe cations in these enzymes.^{2a,3,6} Our model is considerably larger than models used in previous theoretical works examining the interaction of O_2^- with CuZnSOD^{2c} and FeSOD⁹ or FeSOR,^{9,13} where only the first sphere of coordination of the metal centers (ligands in the middle and bottom of Figure 1) was included. As we will show below, this is a severe approximation that misses important features for the bonding of O_2^- to MnSOD and FeSOD enzymes. In our model, the amino acids were initially set at the positions found in the corresponding crystal structures. Then, during the DF calculations, the amino acids were allowed to relax, keeping the position of the atoms that link them to the enzyme backbone fixed. Our model does not include solvation effects, but it is similar to models that recently have been very useful for examining the physical and chemical properties of MnSODs and FeSODs.^{6b} The existing experimental evidence indicates that solvation effects do not play an important role for the systems under study here.^{1c,2a,3,6} The metal centers of manganese and iron SODs are surrounded by amino acids in such a way that water cannot get close to a bound O_2^- molecule.^{2a,3,6} The crystal structures show only one water molecule in the second sphere of coordination, and this was included in our model (see top of Figure 1). The water molecule

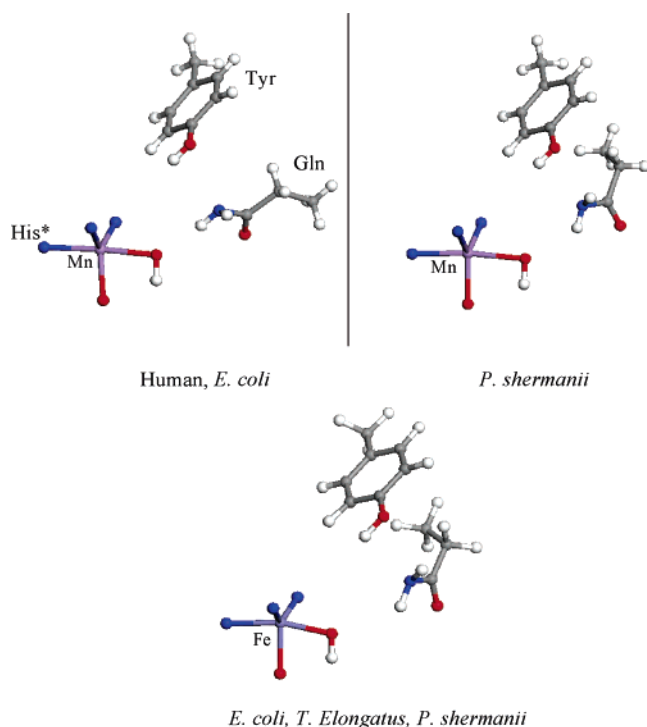


Figure 2. (top) Position of the tyrosine and glutamine ligands around the metal center in MnSODs. A similar configuration is observed for the human and *E. coli* enzymes, while in the cambialistic *P. shermanii* the position of the glutamine is different.^{24–26} (bottom) Position of the tyrosine and glutamine ligands around the metal center in FeSODs (*E. coli*, *T. elongatus*, and cambialistic *P. shermanii*).^{5b,26,27} The different colors denote the following: magenta, Mn; light blue, Fe; gray, carbon; white, hydrogen; dark blue, nitrogen; red, oxygen. For simplicity, the first sphere of coordination around the metal centers is not shown (see Figure 1).

was free to move during geometry optimization and did not approach the O_2^- attached to the Mn or Fe sites. Experimental studies show that changes in pH have no effect on the catalytic activity of MnSODs over a broad pH range,^{1c} consistent with the fact that the active centers in these enzymes are not exposed to the water solvent.

Results

A. Structural Properties of MnSODs and FeSODs. Following previous studies,^{5d} we start by examining the reported crystal structures of MnSODs present in human cells²⁴ and *Escherichia coli*,²⁵ plus the Mn-bound cambialistic SOD from *Propionibacterium shermanii*.²⁶ In the oxidized systems, the Mn has a +3 formal oxidation state and a high spin ($S = 2$).⁹ The Mn(III) cation is bonded to three histidines, one aspartate, and, as suggested in recent literature, an OH group.⁶ For the reduced enzymes, the Mn has a formal oxidation state of +2, has a high spin ($S = 5/2$), and is bonded to an H_2O molecule instead of an OH group.⁶ A close examination of the crystal structures of the MnSODs reveals subtle yet important differences in the positions of the tyrosine and glutamine amino acids in the second sphere of coordination (Figure 2, top left). For example, in the human MnSOD the glutamine points directly toward the Mn center, with a relatively short Mn–N_{Gln} distance (~ 4.5 Å).²⁴ For the *E. coli* MnSOD, the Mn–N_{Gln} separation is larger (~ 4.65 Å).²⁵ Finally, in the case of the *P. shermanii* MnSOD, one sees a different orientation for the glutamine (Figure 2, top right) and a relatively big Mn–N_{Gln} distance (~ 4.8 Å).²⁶ In our DF calculations we relaxed the geometries of the Mn centers and their ligand neighbors, obtaining structural parameters very

TABLE 1: Human Mn(III)SOD: Comparison of Optimized and Experimental Bond Distances (Å)

	DFT results	XRD results ^a
Mn–O(water) ^b	2.11	2.08
Mn–N(His163)	2.08	2.07
Mn–N(His26)	2.05	2.09
Mn–N(His74)	2.09	2.07
Mn–O(Asp159)	1.98	1.94

^a From ref 24. ^b A distance of 1.91 Å was calculated when Mn(III) was bonded to an OH group.

TABLE 2: *E. coli* Fe(III)SOD: Comparison of Optimized and Experimental Bond Distances (Å)

	DFT results	XRD results ^a
Fe–O(OH)	1.90	1.92
Fe–N(His160)	2.09	2.08
Fe–N(His26)	2.11	2.15
Fe–N(His73)	2.08	2.06
Fe–O(Asp156)	1.92	1.89

^a From ref 5b.

similar to those found in X-ray diffraction (XRD) measurements^{24–26} and in previous theoretical studies.^{8a} Typical results are shown in Table 1.

For FeSODs, we compared the crystal structures of enzymes found in *Escherichia coli*,^{5b} *Propionibacterium shermanii* (Fe-bound cambialistic SOD),²⁶ and the thermophilic cyanobacterium *Thermosynechococcus elongatus*.²⁷ In the oxidized state of the enzymes, Fe has a +3 formal oxidation state, high spin ($S = 5/2$),^{9,10} and a set of neighbors identical to that described above for the MnSODs.²⁸ For the reduced state of these systems, iron has a +2 oxidation state and high spin ($S = 2$).^{9,10} In the three FeSODs examined, the positions of the tyrosine and glutamine amino acids are equivalent (Figure 2, bottom). The Fe–N_{Gln} distance is ~ 4.55 Å in the *P. shermanii* FeSOD, and increases to ~ 5.05 Å in the *T. elongatus* FeSOD and ~ 5.1 Å in the *E. coli* FeSOD. After relaxing the geometries of the Fe centers and their ligands, our DF calculations yielded bond distances and angles that match reasonably well those found in XRD studies^{5b,26,27} and other theoretical works.³ The good agreement observed in Table 2 for experiment and theory is typical.

The FeSODs of the *E. coli* and *T. elongatus* display a second sphere of coordination around the metal center that is structurally different from that seen in the MnSODs of human cells and *E. coli*:^{5b,5d,24,25,27} The glutamine is well separated from the metal center in the FeSODs. A similar difference was noticed in a previous work after comparing the crystal structures of the *E. coli* FeSOD and the *T. thermophilus* MnSOD.^{5d} The greater distance between the glutamine and the Fe(III) cation probably reduces the participation of the amino acid in hydrogen bonding.^{5c} Interestingly, the Mn and Fe forms in the cambialistic SOD from *P. shermanii* show similar structures.²⁶ They can be seen as an intermediate case between the standard MnSODs^{24,25} and FeSODs.^{5b,27}

B. Protonation of OH Ligand in Mn(III)SOD and Fe(III)SOD. In the oxidized forms of the MnSODs and FeSODs, the cations have a +3 formal charge and are probably bound to a hydroxide ligand (see Figure 1).⁶ In principle, the OH ligand could react with a proton from the medium or an amino acid to form water.^{8,23c} A reaction pathway has been proposed in which the metal-bound OH abstracts a proton from the NH_2 group in the nearby glutamine or the OH group in the tyrosine.^{23c} Our DF calculations indicate that such a pathway is highly endothermic for the Mn(III)SODs and Fe(III)SODs. An endothermic

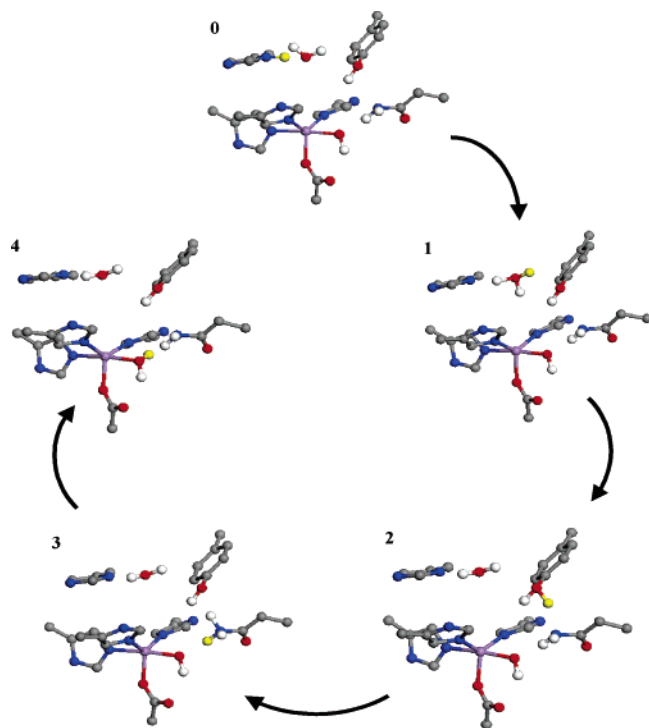


Figure 3. Different steps for the reaction of a proton from the medium with a metal-bound OH group. For simplicity, we are only showing H atoms that are in the direct path for proton transfer within the enzyme. A complete view of our working model is shown in Figure 1. Originally the proton was in the medium as a H_9O_4^+ complex^{23d} (not shown). Once the proton is bound to the histidine in the second sphere of coordination (step 0), the proton transfer within the enzyme starts. In the final step, the metal-bound OH has been transformed into water.

reaction was also found when the proton abstraction involved SOD enzymes with Mn(II)–OH and Fe(II)–OH units. These proton transfers are uphill due to $\text{p}K_{\text{a}}$'s of the glutamine and tyrosine amino acids that are substantially above neutral.²⁹ A second possibility that must be considered is reaction of the metal-bound OH with a proton from the medium. Since the Mn(III) and Fe(III) centers are surrounded by a network of amino acids, the proton from the medium probably follows the pathway shown in Figure 3. Initially this proton moves from the medium, where it is present as a H_9O_4^+ complex^{23d} (initial step, "HP" in our notation), and binds to the histidine in the second sphere of coordination ("0" in our notation), and from there transfers to the water molecule (1), to the tyrosine (2), to the glutamine (3), and finally to the metal-bound OH (4). The calculated energy changes (ΔE) for this proton transfer in human Mn(III)SOD and the *E. coli* Fe(III)SOD are shown in the top panel of Figure 4. The overall reaction is almost thermoneutral for Mn(III)SODs and Fe(III)SODs, but there are substantial energy barriers associated with the proton transfer around the tyrosine. The protonation of the tyrosine from the medium (HP \rightarrow 2) has a ΔE of $\sim +8$ kcal/mol. In addition to this thermodynamic barrier, our calculations estimate that the transition state for the 1 \rightarrow 2 proton transfer is more than 14 kcal/mol above the protonated tyrosine. The total barriers (thermodynamic + kinetic > 22 kcal/mol) make the reaction pathway displayed in Figure 3 very difficult. The results of our calculations are consistent with models that propose that in the resting forms of the oxidized MnSODs and FeSODs the metal centers are bound to an OH group and no water.⁶

For the human Mn(III)SOD, we also investigated the effect of replacing the tyrosine by a phenylalanine (Y34F mutation). The bottom panel in Figure 4 compares the calculated energy

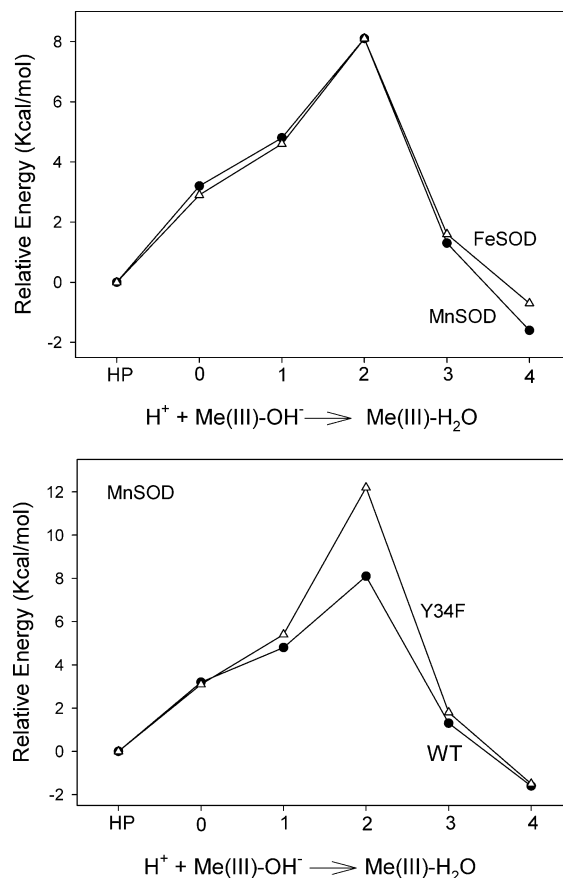


Figure 4. (top) Calculated energy changes for a proton transfer from the medium to the metal-bound OH in the human Mn(III)SOD and the *E. coli* Fe(III)SOD. The individual steps for this proton transfer are shown in Figure 3. In the initial (and reference) state, the proton is present in the medium as a H_9O_4^+ complex^{23d} (HP in our notation). From here, it moves to the histidine in the second sphere of coordination around the metal center (step 0 for the proton transfer within the enzymes). (bottom) Corresponding energy changes for a Y34F mutation in the human Mn(III)SOD. Only thermodynamic values are shown; no kinetic barriers are included (see text).

changes for the proton transfer in the wild-type and mutant enzymes. The Tyr \rightarrow Phe substitution significantly enhances the energy barrier and makes the transformation of the metal-bound OH into water thermodynamically very unlikely. As we will see below, this transformation is facilitated by the binding of O_2^- to the Mn(III) and Fe(III) cations.

C. Bonding of O_2^- to MnSODs and FeSODs. We address first the binding of O_2^- to Mn(II) and Mn(III) cations as given in reactions 2–5.^{6,7,23c} In the Mn(II)– O_2^- systems, a large overlap between the singly occupied molecular orbital (SOMO) of the O_2^- anion and the proper t_{2g} and e_g SOMOs of the metal ion makes an $S = 2$ state more stable than an $S = 3$ state.⁹ A partial electron transfer from O_2^- to Mn(III) makes an $S = 5/2$ state more stable than an $S = 3/2$ state in the Mn(III)– O_2^- systems.

In principle, O_2^- can bind to the metal centers of MnSODs via end-on (one Mn–O bond) or side-on (two Mn–O bonds) conformations.^{9,11–13,30} In fact, it has been suggested that a side-on conformation could be involved in the formation of an inactive complex during the reaction of superoxide with reduced Mn(II)SOD.³⁰ This hypothesis is not supported by the results of our DF calculations, which show that side-on conformations are not stable (i.e., no local minima) and spontaneously transform into end-on conformations. On one hand, side-on conformations are not favored by the high coordination number

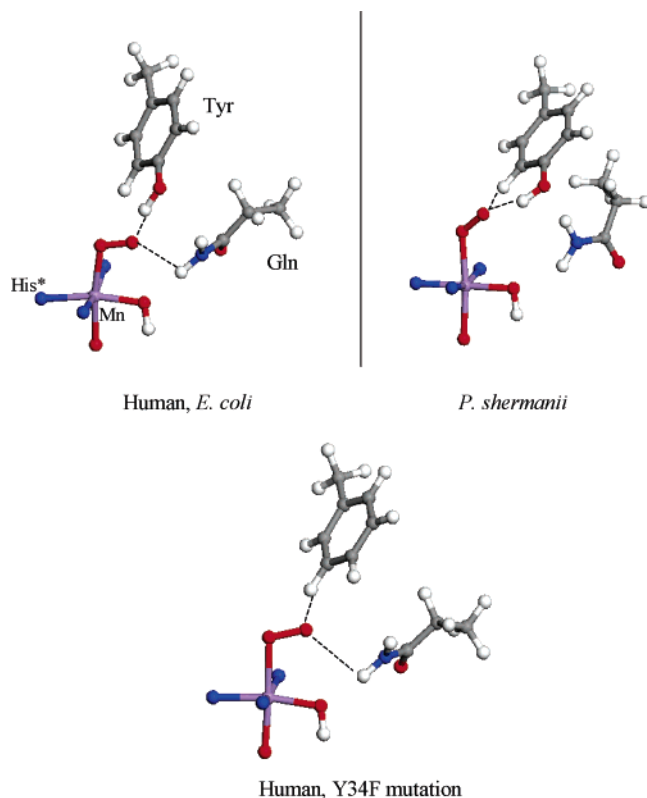


Figure 5. (top) Preferred bonding configuration for O_2^- on MnSODs. In the human and *E. coli* enzymes, the O_2^- is H bonded (dashed lines) with the tyrosine and glutamine in the second sphere of coordination. For the cambialistic *P. shermanii*, the O_2^- interacts only with the Mn cation and the tyrosine. (bottom) Preferred bonding configuration for O_2^- on a Y34F mutation (tyrosine to phenylalanine) of the human MnSODs. The different colors denote the following: magenta, Mn; gray, carbon; white, hydrogen; dark blue, nitrogen; red, oxygen. Dashed lines are used to represent H bonding. Not shown is the bonding configuration for O_2^- on FeSODs, which is similar to that found for O_2^- on the Mn form of the cambialistic *P. shermanii*.

of the Mn(II) and Mn(III) cations. On the other hand, in end-on conformations the free atom of the bound O_2^- molecule can form hydrogen bonds with the tyrosine and glutamine amino acids in the second spheres of coordination in human, *E. coli*, and Y34F human mutant MnSODs; see Figure 5. In contrast, the hydrogen bonding forms only between the superoxide and the tyrosine in the Mn-bound *P. shermanii* as the glutamine here is too far away for H bonding. When the second sphere of coordination in Figure 1 was removed, the side-on conformation was still not stable, and an end-on conformation with the free oxygen of the bound O_2^- forming hydrogen bonds with a CH in one of the histidine ligands (His26 for the manganese enzymes, “His*” in our notation) was observed. This bonding configuration became a local minimum after adding the second sphere of coordination because it is 4–5 kcal/mol less stable than the bonding configuration shown at the top of Figure 5.

Figure 6 shows calculated bonding energies for O_2^- with the MnSODs. Due to electrostatic interactions, the superoxide anion bonds better to Mn(III) than to Mn(II). The DF calculations indicate that the second sphere of coordination plays an important role in the binding of O_2^- to the enzymes through H bonding, especially in the case of Mn(II)– O_2^- systems. For example, when the second sphere of coordination was removed from our model shown in Figure 1, the bonding energy of O_2^- to a human Mn(II)SOD decreased from –12.8 to –8.9 kcal/mol (~30%). The variations in O_2^- bonding energy seen in Figure 6 for the wild types of the human, *E. coli*, and

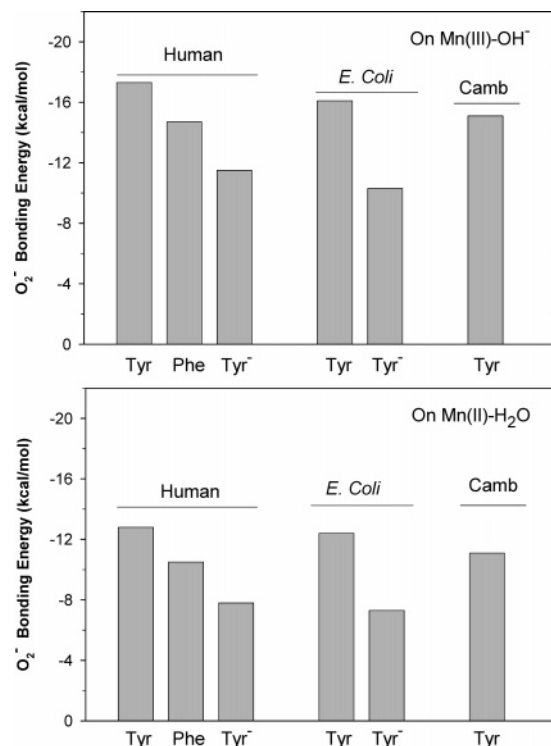


Figure 6. Calculated bonding energies for O_2^- on MnSODs. The graph shows results for O_2^- bonding to the wild type (Tyr label), wild type with a deprotonated tyrosine (Tyr⁻ label), and a Y34F mutation in the human enzyme (Phe label). (top) Mn(III); (bottom) Mn(II).

TABLE 3: Interaction of O_2^- with Second Sphere of Coordination: Bond Distances (Å)

	O···HOTyr	O···HTyr	O···HGln
Mn(III)SOD			
human	1.49	2.04	2.34
<i>E. coli</i>	1.60	1.92	2.58
cambialistic	1.77	1.83	3.34
Fe(III)SOD			
<i>T. elongatus</i>	1.79	1.70	3.58
<i>E. coli</i>	1.84	1.69	3.60
cambialistic	1.74	1.75	3.39

cambialistic *P. shermanii* are a consequence of changes in the strength of the H bonding between the O_2^- anion and the tyrosine and glutamine in the second sphere of coordination. As the tyrosine and glutamine shift away from the Mn center and O_2^- (see Table 3), the O_2^- bonding energy is reduced.

Mutation of the tyrosine into a phenylalanine is known to have a significant effect in the mechanism of the dismutation of O_2^- in MnSODs.³¹ In the corresponding models we performed a tyrosine to phenylalanine switch and observed a small reduction in the O_2^- bonding energy (Figure 6) and a shift in the position of the bound O_2^- (bottom of Figure 5). With the lack of hydrogen bonding to the HO of a tyrosine, this configuration is now only ca. 2 kcal/mol more stable than a configuration in which superoxide is rotated 180° and hydrogen bonded to a CH in His*. Eventually these changes could lead to variations in the rates for trapping and protonation of O_2^- .

Now, we focus our attention on the interaction of O_2^- with oxidized and reduced FeSODs. A strong interaction of the SOMO of O_2^- with the occupied d orbitals of Fe(II) makes an $S = 5/2$ state more stable than an $S = 3/2$ state in the Fe(II)– O_2^- systems.⁹ For the Fe(III)– O_2^- systems, a partial electron transfer from O_2^- to Fe(III) leads to an $S = 2$ ground state. In all cases we found that O_2^- was more stable bound in an end-

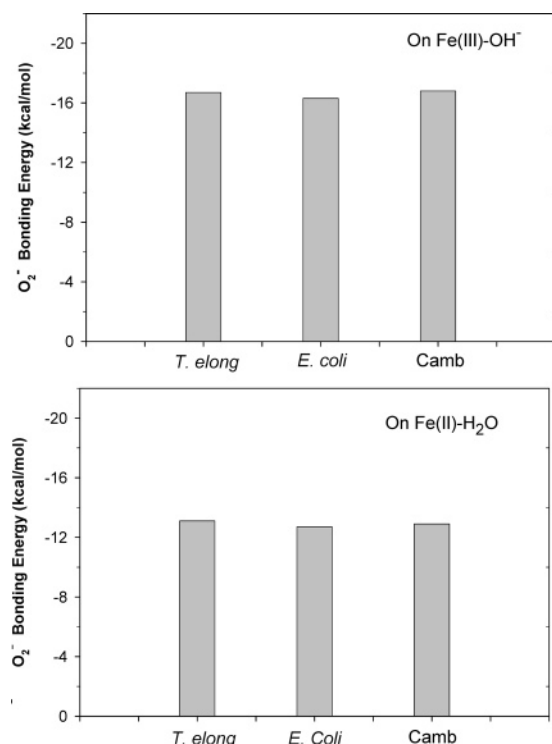
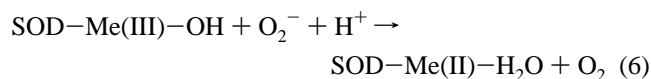


Figure 7. Calculated bonding energies for O₂⁻ on FeSODs. The graph shows results for O₂⁻ bonding to the wild types of the human, *E. coli*, and cambialistic *P. shermanii* enzymes. (top) Fe(III); (bottom) (Fe(II).

on conformation than in a side-on conformation. Figure 7 shows the calculated bonding energies for O₂⁻ to the FeSODs. The O₂⁻ bonding energies with Fe(III) are stronger than those with Fe(II). For the enzymes in Figure 7 the second sphere of coordination around the metal has a similar structural geometry (see bottom of Figure 2) and, thus, the variations in O₂⁻ bonding energy are small (<0.6 kcal/mol). Hydrogen bonding occurs between the bound O₂⁻ and the tyrosine amino acid, but the glutamine is too far away for an effective bonding interaction (Table 3). When the second sphere of coordination was removed from our working model shown in Figure 1, the O₂⁻ bonding energy to *E. coli* Fe(II)SOD decreased from -12.7 to -10.9 kcal/mol (~15%).

A comparison of the DF results for the Mn and Fe forms of the cambialistic *P. shermanii*, enzymes that have a similar second sphere of coordination (Figure 5), shows that the Fe cations bind O₂⁻ more strongly than the Mn cations. This is also valid for the Fe- and MnSODs of *E. coli*, even with a negligible participation of the glutamine of the FeSOD in hydrogen bonding to the O₂⁻. The higher chemical activity of the iron centers makes the FeSODs less dependent on the structure of the second sphere of coordination than the MnSODs.

D. Reduction of Mn(III)SODs and Fe(III)SODs with O₂⁻ and H⁺. The first step in the catalytic dismutation of O₂⁻ anions by MnSODs and FeSODs involves the reduction of the enzyme metal centers:



Experimental studies have not been able to provide the details of the mechanism for this reaction.^{1,3,5-7} Previous DF calculations indicate that a transformation of the metal-bound OH into water by reaction with a proton is a preliminary step for an electron transfer from O₂⁻ to the Mn(III) or Fe(III) cations,^{23c}

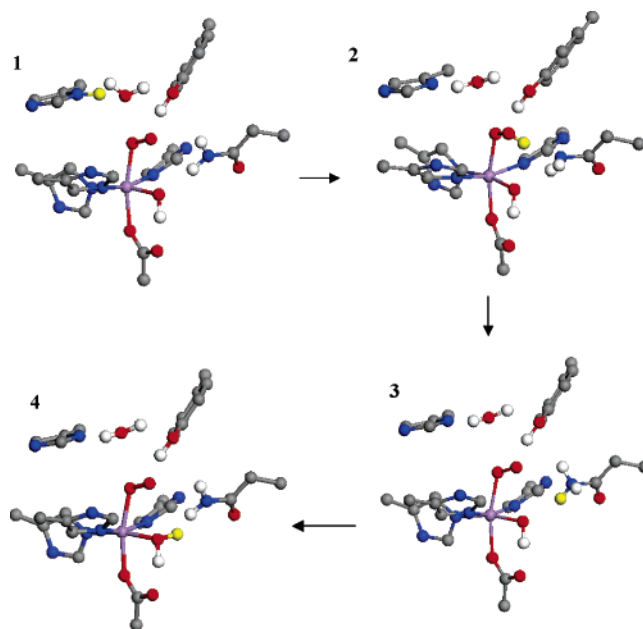


Figure 8. Different steps for the transfer of a proton from the medium to a metal-bound OH group via a metal-bound O₂⁻. For simplicity, we are only showing H atoms that are in the direct path for proton transfer. A complete view of our working model is shown in Figure 1. In the initial step (0 in our notation), the proton is bound to the histidine in the second sphere of coordination. In the final step, the metal-bound OH has been transformed into water.

but the source of the proton and its pathway to reach the metal-bound OH were not well-defined. It was proposed that the required proton could come from the glutamine or tyrosine in the second sphere of coordination around the metal.^{23c} This hypothesis seems to be inconsistent with the high pK_a's for these amino acids.²⁹ Our DF calculations show that such proton transfer is uphill with or without the O₂⁻ interacting with the Mn(III) and Fe(III) centers. The proton for reaction 6 could come from the medium, and could approach the metal-bound OH following either the pathway shown in Figure 3 (but now with O₂⁻ also bound to the metal) or the pathway displayed in Figure 8. In the pathway of Figure 8, the proton is initially attached to the top histidine, then moves to the O₂⁻ bound to the metal, and from there could jump to the glutamine or directly to the metal-bound OH, bypassing the tyrosine altogether.

We calculated the energy changes associated with both pathways for H⁺ transfer. Figure 9 shows the specific results for the human Mn(III)SOD, top panel, and the *E. coli* Fe(III)SOD, bottom panel. In all the systems examined, we found that the O₂⁻ bound to the metal opened a new pathway for proton transfer. This pathway shows no significant energy barrier for proton transfer, and should be preferred over the pathway via the tyrosine (Figure 3). The fact that the O₂⁻ binds to Mn(III) and Fe(III) in end-on configurations is crucial for the energetics of proton transfer and the reduction of these metal centers. In agreement with earlier DF calculations,^{23c} we found that a transformation of the metal-bound OH into water by reaction with a proton is a necessary step for an electron transfer from O₂⁻ to the Mn(III) or Fe(III) cations (i.e., proton-assisted electron transfer).

Figure 10 displays the energy changes occurring for proton transfer in a Y34F mutation of the human Mn(III)SOD. Once again, a proton transfer via the bound O₂⁻ is energetically more favorable. Interestingly, without this pathway, reaction 6 will never occur in a Y34F mutation, because the channel for proton transfer via the phenylalanine has a very large energy barrier.

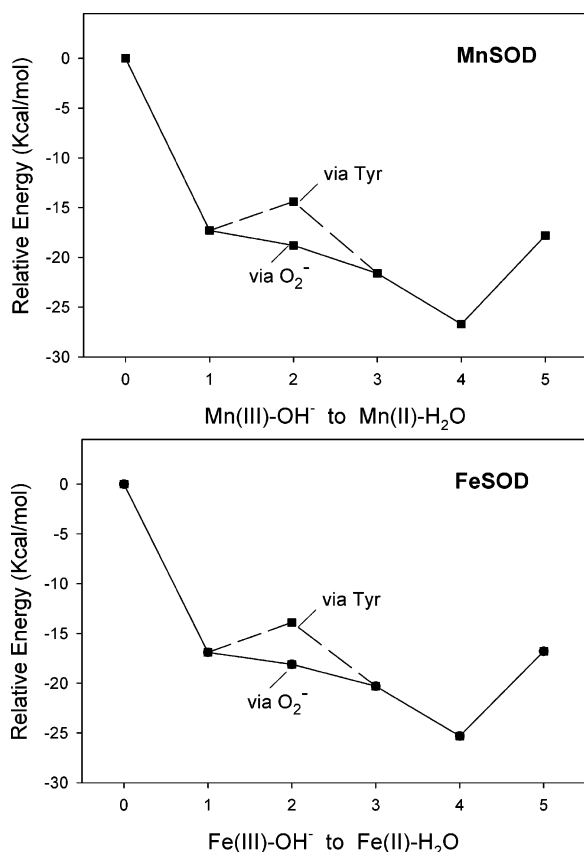


Figure 9. Calculated energy changes for a proton transfer from the medium to the metal-bound OH in the human Mn(III)SOD (top) and the *E. coli* Fe(III)SOD (bottom). Some of the individual steps for this proton transfer are shown in Figure 8. In the reference state (0 in our notation), the proton from the medium is attached to the histidine in the second sphere of coordination for the metal center and the O₂⁻ is not bound. In step 1, the O₂⁻ binds to the Mn(III) or Fe(III) center. In step 2, a proton moves from the histidine to the bound O₂⁻ (solid lines) or to the tyrosine (dashed lines). In steps 3 and 4, the proton goes to the glutamine and metal-bound OH, respectively. In the last step (5), an O₂ molecule is released from the metal centers.

The pathway for proton transfer through the bound O₂⁻ essentially makes the rate for reaction 6 insensitive to mutations of the tyrosine.

Discussion

From previous works, it is not clear if O₂⁻ binds to the metal centers of MnSODs and FeSODs via end-on (one Mn–O or Fe–O bond) or side-on (two Mn–O or Fe–O bonds) conformations.^{1,5a,9,11–13} The way in which the molecule binds to the metal centers can affect the rate of subsequent protonation and determine the mechanism for the formation of H₂O₂ in reactions 4 and 5. Our DF studies show that the most stable configuration of the bound superoxide in both the oxidized and reduced metal centers of the enzymes is end-on and hydrogen bonded to the tyrosine (and glutamine in the case of the MnSODs) in the second sphere of coordination. A recent publication on anion binding in FeSOD postulated that superoxide sits end-on between the tyrosine proton and the iron and further suggested that an azide ligand (N₃⁻) is too large and a F⁻ ligand is too small to have the same stabilization.³² This is consistent with our calculations.³²

In a recent work it has been proposed that the loss of the proton bound to oxygen in the tyrosine amino acid is responsible for the deactivation of the *E. coli* MnSOD at high pH.^{3,6} Our

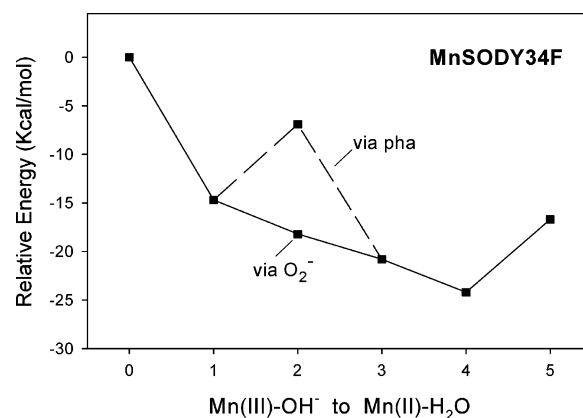


Figure 10. Calculated energy changes for proton transfer in a Y34F mutation for the human Mn(III)SOD. For a detailed explanation of the different steps, see the caption of Figure 9. In step 2, a proton moves from the histidine in the second sphere of coordination to the bound O₂⁻ (solid lines) or to the phenylalanine (dashed lines).

results indicate that the removal of the proton from the tyrosine diminishes H bonding and introduces an electrostatic repulsion between the negative O end of the amino acid and the O₂⁻. After the removal of the proton from the tyrosine, the O₂⁻ bonding energy decreases substantially (Figure 6), and this could have a significant impact on the rates of reactions 2–5. It is important, however, to realize that the removal of the proton from the tyrosine can vary in a complex way with pH for each enzyme,³³ depending on subtle changes to the overall structures of the different MnSODs and access to the active site channel. Thus far, it is impossible to unequivocally assert that the high pH pK results from deprotonation of the tyrosine and not from a histidine near the active site.

The FeSODs of *E. coli* and *T. elongatus* display a second sphere of coordination around the metal center that is structurally different from that seen in the MnSODs of human cells and *E. coli*. The higher chemical reactivity that is intrinsic to an iron center versus a manganese center makes the FeSODs less dependent on the structure of the second sphere of coordination than the MnSODs. This could help to explain the position of the glutamine in the FeSODs of *T. elongatus*, *E. coli*, or *P. shermanii*, and the absence of this amino acid in the second sphere of coordination of some other FeSODs.²⁶

The results in Figure 4 show that there is a substantial energy barrier for the protonation of the OH group bound to the metal center in oxidized Mn(III)SOD or Fe(III)SOD, but the overall protonation process is energetically downhill. Thus, the wild types of these enzymes in the resting state should contain an OH group (as suggested in the literature⁶), but a mutation of the tyrosine in the second sphere of coordination could reduce the energy barrier and facilitate the protonation of the OH group to form a water ligand. This is not the case for a tyrosine → phenylalanine mutation (see Figure 4), but it could happen if an amino acid that helps proton transfer (histidine, glutamine, etc.) replaces the tyrosine. Clearly, what is required here is an amino acid residue that is both a good proton transfer agent and is close enough to be in the second sphere of coordination or space for a water to occupy this location and act as a proton transfer agent.

The DF calculations indicate that the proton transfer in reaction 6, which is reduction of the metal by superoxide radical, probably does not need to involve the tyrosine and glutamine in the second sphere of coordination around the metal centers of the SODs. The presence of the O₂⁻ bound to Mn(III) or Fe(III) opens the possibility for a direct proton transfer to the OH

ligand. This is in contrast with previously proposed reaction pathways that suggest the involvement of both of these amino acid residues,^{23c} but is consistent with experimental data that show negligible changes in the reaction rate (the so-called k_1) when the tyrosine or glutamine amino acids are mutated.³¹ For example, if the tyrosine is involved in the pathway for proton transfer as suggested,^{23c} then a tyrosine \rightarrow phenylalanine mutation should lead to a large reduction in the rate of reaction 6. No such effect is seen in the experimental measurements.³¹

The mechanism for the dismutation of O_2^- in human and *E. coli* MnSODs involves two parallel pathways for the reaction of Mn(II)SOD with superoxide while only one pathway, corresponding to reactions 3 and 4, has been observed in FeSODs.^{2,5,7} The extra step seen in the MnSODs may be associated with the position of the glutamine amino acid in the second sphere of coordination.^{2a,7} The results in section C show that the glutamine in the MnSODs is not an innocent spectator. The position of the glutamine could slow the rate of protonation and removal of O_2^{2-} from the metal center in reactions 4 and 5. This is currently being investigated.

Conclusions

Superoxide binding to both MnSODs and FeSODs, regardless of origin, is preferentially in the end-on and not the side-on conformation. In all cases, the superoxide binding is stabilized by hydrogen bonding with the tyrosine in the second coordination sphere and, in the case of the human and *E. coli* MnSODs, by hydrogen binding with the glutamine in the second coordination sphere as well. There is a thermodynamic barrier to proton transfer to the bound hydroxide on the metal center in both MnSOD and FeSOD that arises from the tyrosine. However, and most importantly, when superoxide is bound to the metal the barrier is lowered, enabling a facile and thermodynamically favored proton transfer as part of the electron transfer process. Additionally, any change of the tyrosine raises the barrier to proton transfer, making superoxide binding an exclusive pathway for proton transfer to the bound hydroxide.

Acknowledgment. This research was supported by LDRD funds at Brookhaven National Laboratory, the National Institutes of Health (Grant GM54903), and the U.S. Department of Energy (DE-AC02-98CH10086). The authors acknowledge helpful discussions with Prof. David Silverman (University of Florida, Gainesville).

Supporting Information Available: Cartesian coordinates for the active site of the human Mn(III)SOD enzyme, and for the O_2^- bound to this center, are available free of charge via the Internet at <http://pubs.acs.org>. For the active sites of other enzymes, the coordinates can be obtained in different formats upon request to the authors.

References and Notes

- (1) (a) Miller, A.-F.; Sorkin, D. L. *Comments Mol. Cell. Biophys.* **1997**, 9, 1. (b) Miller, A.-F.; Padmakumar, K.; Sorkin, D. L.; Karapetian, A.; Vance, C. K. *J. Inorg. Biochem.* **2003**, 93, 71. (c) Cabelli, D. E.; Riley, D.; Rodriguez, J. A.; Valentine, J. S.; Zhu, H. Models of Superoxide Dismutase. In *Biomimetic Chemistry*; Meunier, B., Ed.; Imperial College Press: London, 2000; pp 461–508 and references therein.
- (2) (a) L  v  que, V. J.-P.; Stroupe, M. E.; Lepock, J. R.; Cabelli, D. E.; Tainer, J. A.; Nick, H. S.; Silverman, D. N. *Biochemistry* **2000**, 39, 7131. (b) Getzoff, E. D.; Cabelli, D. E.; Fisher, C. L.; Parge, H. E.; Viezzoli, M. S.; Banci, L.; Hallewell, R. A. *Nature* **1992**, 358, 347. (c) D'Alessandro, M.; Aschi, M.; Paci, M.; Di Nola, A.; Amadei, A. *J. Phys. Chem. B* **2004**, 108, 16255.
- (3) (a) Jackson, T. A.; Brunold, T. C. *Acc. Chem. Res.* **2004**, 37, 461. (b) Bull, C.; Fee, J. A. *J. Am. Chem. Soc.* **1985**, 107, 3295.
- (4) *Superoxide Dismutase*; Packer, L., Ed.; Methods in Enzymology 349; Academic Press: San Diego, 2002.
- (5) (a) Whitaker, J. W. *Biochem. Soc. Trans.* **2003**, 31, 1318. (b) Lah, M. S.; Dixon, M. M.; Patridge, K. A.; Stallings, W. C.; Fee, J. A.; Ludwig, M. L. *Biochemistry* **1995**, 34, 1646. (c) Hunter, T.; Bannister, J. V.; Hunter, G. J. *Eur. J. Biochem.* **2002**, 269, 5137. (d) Jackson, S. M. J.; Cooper, J. B. *BioMetals* **1998**, 11, 159. (e) Schwartz, A. L.; Yikilmaz, E.; Vance, C. K.; Vathyam, S.; Koder, R. L.; Miller, A. F. *J. Inorg. Biochem.* **2000**, 80, 247.
- (6) (a) Maliekal, J.; Karapetian, A.; Vance, C.; Yikilmaz, E.; Wu, Q.; Jackson, T.; Brunold, T. C.; Spiro, T. G.; Miller, A.-F. *J. Am. Chem. Soc.* **2002**, 124, 15065. (b) Jackson, T. A.; Karapetian, A.; Miller, A.-F.; Brunold, T. C. *J. Am. Chem. Soc.* **2004**, 126, 12477.
- (7) Hsieh, Y.; Guan, Y.; Tu, C.; Bratt, P. J.; Angerhofer, A.; Lepock, J. R.; Hickey, M. J.; Tainer, J. A.; Nick, H. S.; Silverman, D. N. *Biochemistry* **1998**, 37, 4731.
- (8) (a) Li, J.; Fisher, C. L.; Konecny, R.; Bashford, D.; Noodleman, L. *Inorg. Chem.* **1999**, 38, 929. (b) Han, W.-G.; Lovell, T.; Noodleman, L. *Inorg. Chem.* **2002**, 41, 205. (c) Liu, X. H.; Sun, M.; Yue, J. J.; Yin, Y. X.; Liu, X. L.; Miao, F. M. *J. Mol. Struct.* **2003**, 620, 227.
- (9) Carrasco, R.; Morgenstern-Badarau, I.; Cano, J. *Chem. Commun.* **2003**, 436.
- (10) Renault, J. P.; Verch  re-B  aur, C.; Morgenstern-Badarau, I.; Yamakura, F.; Gerloch, M. *Inorg. Chem.* **2000**, 39, 2666.
- (11) (a) Castej  n, H.; Hern  ndez, A. J.; Ruet  , F. *J. Phys. Chem.* **1988**, 92, 4970. (b) Huber, H.; Ozin, G. A. *Can. J. Chem.* **1972**, 50, 3746. (c) Hern  ndez, A. J.; Ruet  , F.; Lude  a, E. V. *J. Mol. Catal.* **1987**, 39, 21. (d) Valentine, J. S. *Chem. Rev.* **1973**, 73, 235.
- (12) Rodriguez, J. A.; Abreu, I. A. *J. Phys. Chem. B* **2005**, 109, 2754.
- (13) Silaghi-Dumitrescu, R.; Silaghi-Dumitrescu, I.; Coulter, E. D.; Kurtz, D. M. *Inorg. Chem.* **2003**, 42, 446.
- (14) (a) Delley, B. *J. Chem. Phys.* **1990**, 92, 508. (b) Delley, B. *J. Chem. Phys.* **2000**, 113, 7756.
- (15) Rodriguez, J. A.; Liu, P.; Dvorak, J.; Jirsak, T.; Gomes, J.; Takahashi, Y.; Nakamura, K. *Surf. Sci.* **2003**, 543, L675; *Phys. Rev. B* **2004**, 69, 115414; *J. Chem. Phys.* **2004**, 121, 465.
- (16) Liu, P.; Rodriguez, J. A.; Hou, H.; Muckerman, J. T. *J. Chem. Phys.* **2003**, 118, 7737.
- (17) (a) Maiti, A.; Rodriguez, J. A.; Law, M.; Kung, P.; McKinney, J. R.; Yang, P. *Nano Lett.* **2003**, 3, 1025. (b) Chandra, A. K.; Uchamaru, T. *Int. J. Mol. Sci.* **2002**, 3, 407.
- (18) (a) Schneider, W. F.; Li, W. F.; Hass, K. C. *J. Phys. Chem. B* **2001**, 105, 6972. (b) Miletic, M.; Gland, J. L.; Schneider, W. F.; Hass, K. C. *J. Phys. Chem. B* **2003**, 107, 157. (c) Rodriguez, J. A.; Maiti, A. *J. Phys. Chem. B* **2000**, 104, 3630.
- (19) Becke, A. D. *Phys. Rev. A* **1988**, 38, 3098.
- (20) Wang, Y.; Perdew, Y. P. *Phys. Rev. B* **1991**, 44, 13298.
- (21) Mulliken, R. S. *J. Chem. Phys.* **1955**, 23, 1841.
- (22) (a) Szabo, A.; Ostlund, N. S. *Modern Quantum Chemistry*; McGraw-Hill: New York, 1989. (b) Wiberg, K. B.; Rablen, P. R. *J. Comput. Chem.* **1993**, 14, 1504.
- (23) (a) Baik, M.-H.; Gherman, B. F.; Friesner, R. A.; Lippard, S. J. *J. Am. Chem. Soc.* **2002**, 124, 14608. (b) Hinnemann, B.; N  rskov, J. K. *J. Am. Chem. Soc.* **2004**, 126, 3920; *J. Am. Chem. Soc.* **2003**, 125, 1466. (c) Noodleman, L.; Lovell, T.; Han, W.-G.; Li, J.; Himo, F. *Chem. Rev.* **2004**, 104, 459. (d) Marx, D.; Tuckerman, M. E.; Hutter, J.; Parrinello, M. *Nature* **1999**, 397, 601.
- (24) Borgstahl, G. E. O.; Parge, H. E.; Hickey, M. J.; Beyer, W. F.; Hallewell, R. A.; Tainer, J. A. *Cell* **1992**, 71, 107.
- (25) Edwards, R. A.; Baker, H. M.; Whittaker, M. M.; Whittaker, J. W.; Jameson, G. B.; Baker, E. N. *J. Biol. Inorg. Chem.* **1998**, 3, 161.
- (26) Schmidt, M.; Meier, B.; Parak, F. *J. Biol. Inorg. Chem.* **1996**, 1, 532.
- (27) Kerfeld, C. A.; Yoshida, S.; Tran, K. T.; Yeates, T. O.; Cascio, D.; Bottin, H.; Berthomieu, C.; Sugiura, M.; Boussac, A. *J. Biol. Inorg. Chem.* **2003**, 8, 707.
- (28) In some cases, the crystal structures do not allow distinguishing if the Fe(III) is bonded to an OH group or a water molecule.²⁷ Following previous studies,^{3,6} we assumed that OH is the ligand bound to Fe(III). Water is the ligand for Fe(II).^{3,6}
- (29) *Lange's Handbook of Chemistry*, 13th ed.; Dean, J. A., Ed.; McGraw-Hill: New York, 1985; pp 5-39 and 5-59.
- (30) Bull, C.; Niederhoffer, E. C.; Yoshida, T.; Fee, J. A. *J. Am. Chem. Soc.* **1991**, 113, 4069.
- (31) Guan, Y.; Hickey, M. J.; Borgstahl, G. E.; Hallewell, R. A.; Lepock, J. R.; O'Connor, D.; Hsieh, Y.; Nick, H. S.; Silverman, D. N.; Tainer, J. A. *Biochemistry* **1998**, 37, 4722.
- (32) Miller, A.-F.; Sorkin, D. L.; Padmakumar, K. *Biochemistry* **2005**, 44, 5969.
- (33) Abreu, I. A.; Cabelli, D. E. To be published. The loss of enzymatic activity with increasing pH is more dramatic for the *E. coli* MnSOD than for the human MnSOD.